Resonant Cavity Enhanced Infrared Photodiodes
for Sensing Applications

Andrew R.J. Marshall and Adam P. Craig

Physics department, Lancaster University,
Lancaster, LA1 4YB
UNITED KINGDOM

a.r.marshall@lancaster.ac.uk

ABSTRACT

Absorption spectroscopy to identify infrared absorption fingerprints is a powerful technique for detection of compounds and threats. Currently it is only achievable with large and/or high-cost systems. Resonant cavity enhanced infrared photodiodes offer a route to compact, low cost and low power spectroscopic sensing. Furthermore, an appropriately designed array of resonant cavity photodiodes could be used to sample an incident spectrum with high resolution and replicate spectrometer functionality at the chip scale. This paper introduces resonant cavity enhanced photodiodes, discusses some of their key characteristics and shows how they can be made to sense at wavelengths across the IR and in an integrated array format. Finally, application to the medical application of sensing glucose in a mixture is discussed, as an application testbed to direct further development, including for threat detection in defence and security applications.

1.0 INTRODUCTION

Infrared material spectroscopy often exploits the ability of infrared photons to excite bond resonances in molecules. Importantly, the resonances depend on the precise atomic and bonding structure of a given molecule and are only excited by photons with a specific matching energy. This results in molecule-specific "absorption fingerprints" which can be detected with infrared spectroscopy. Absorption lines corresponding to fundamental resonances are typically found in the wavelength range between 3 and 12 μm, [1] spanning the so called mid and longwave atmospheric transmission bands. At shorter wavelengths, weaker overtone or combination absorption lines are found in the spectral range between approximately 1.5 and 3 μm. Absorption fingerprint spectra are usually measured by a Fourier transform infrared (FTIR) spectrometer; a technology well suited to the spectral range. However, FTIR spectrometers are physically large table top instruments, which depend on moving mirrors, suited to fixed and benign installation environments. To expand the application space of IR spectroscopic sensing, there have been multiple efforts to develop miniaturised technologies which can measure with the required spectral specificity to support discrimination. [2]-[5] Some success has been achieved using frequency tuneable lasers, as a swept wavelength light source, however these remain expensive and relatively power intensive. This paper summarises recent progress in the development of resonant cavity enhanced infrared photodiodes (RCE-PDs) for spectroscopic sensing.

RCE-PDs integrate a resonant cavity around a photodetector making them inherently spectrally selective, whilst also enhancing detectivity.[6] Classically, spectroscopy systems build spectral selectivity and complexity into the light source, using a simpler broadband detector as depicted in Figure 1(a). Exploiting the sharply defined spectral response of RCE-PDs shown in Figure 1(b), to provide the spectral specificity, offers the potential to use a simple "broadband" light source such as an LED or combination of LEDs. We propose that this offers a desirable pathway to low power, miniaturised spectral sensing. Furthermore, by using a novel technique to realise an integrated array of RCE-PDs, with resonance wavelength varying along the array, a spectrometer on a chip can be conceived. Highly integrated chip scale solutions are attractive for harsh environment because they are inherently reliable and robust, able to be sealed, using fewer parts and none which require movement or servicing.
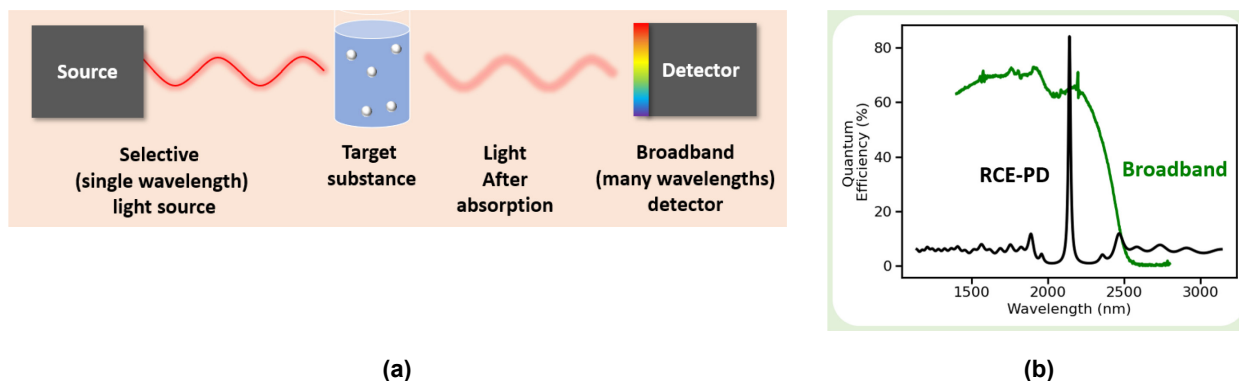
(a)

(b)

Figure 1: (a) Schematic representation of existing spectroscopic sensing systems. (b) Comparison of the spectral responses of conventional broadband detectors and RCE-PD, highlighting their well-defined spectral selectivity.

2.0 ARCHITECTURE AND KEY CHARACTERISTICS OF RCE-PDs

Photodetectors based no III-V semiconductors have been developed to support the full IR spectral range. In particular the family of materials which can be grown on GaSb substrates has become the dominant III-V technology for the ~1.5 - 12 μm range of interest. Mirrors, with defined reflectivities, are required to form an RCE-PD; epitaxially grown distributed Bragg reflectors (DBRs) are well suited to this application. After some earlier attempts to exploit the well-known but lattice-mismatched GaAs/AlGaAs DBR system, [7] researchers have developed AlAsSb/GaSb DBRs, [8] which can be grown lattice matched with GaSb substrates and associated narrow bandgap alloys used to achieve the infrared absorption. The structure of an RCE-PD is shown in Figure 2, with the schematic structure complemented by a cross-sectional SEM image of an actual RCE-PD device. The schematic view illustrates the enhancement of optical field in the absorber, for the resonance wavelength; the core effect behind the spectral selectivity and sensitivity enhancement achievable in RCE-PDs.
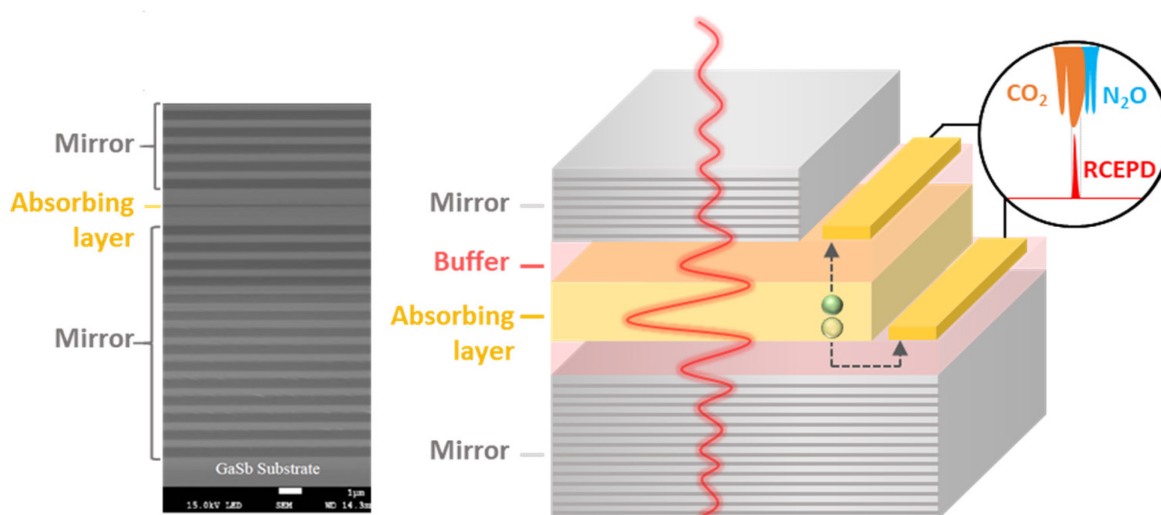

Figure 2: (Right) Schematic of a generic RCE-PD structure, illustrating the enhanced optical field at the resonance wavelength and the flow of photocurrent (layers not to scale). (Left) Cross-sectional SEM image showing the epilayers within a typical RCE-PD.

2.1   Spectral Selectivity and Resonant Field Enhancement

The formation of a cavity and enhancement of the optical field when excited by an appropriate wavelength, are readily understandable requirements for an RCE-PD. However, DBR based RCE-PDs are not simple Fabry Perot cavities and unlike many resonant optical devices they are inherently damped; characteristics which merit further discussion.

Spectral selectivity in DBR based RCE-PDs is primarily driven by the phase shift introduced on reflection for the DBR mirrors, with the optical path length in the cavity only a second order contributor. The phase shift on reflection is itself dependent on the optical path length of the nominally $\lambda/4$ thick DBR layers. Figure 3(a) shows a calculation of this phase shift, for an AlAsSb/GaSb DBR, designed with a centre wavelength of 2000nm. Obviously a non-zero cumulative phase shift reduces the field in the cavity and commensurate sensitivity enhancement. The design of the DBR mirror, refractive index contrast, number of repeats, etc., determines the phase shift vs. wavelength characteristic, and hence defines the spectral width (FWHM) or selectivity of the RCE-PD.


(a)   **(b)**
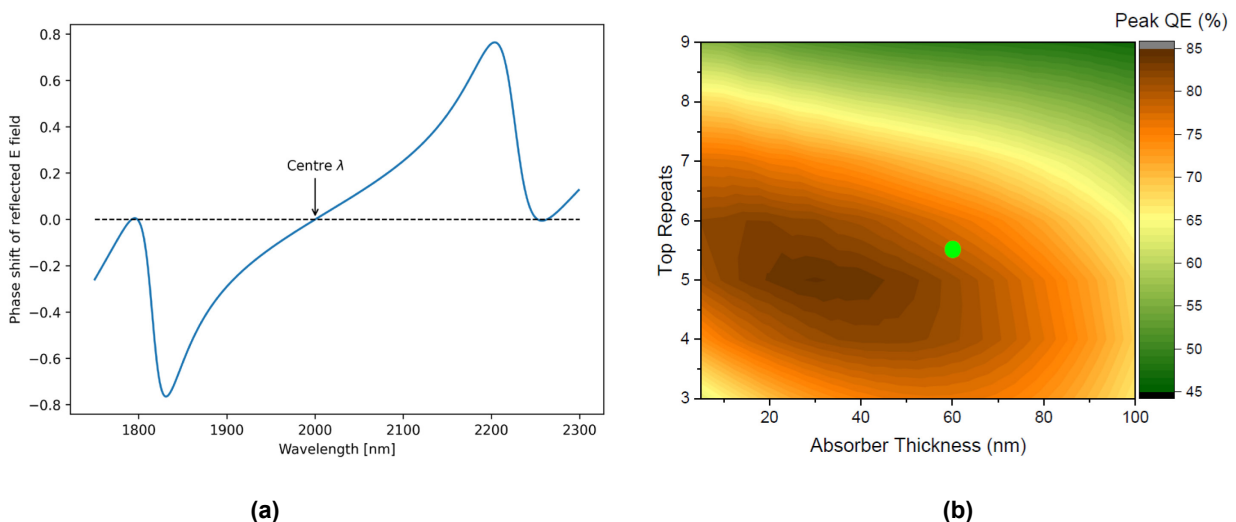
Figure 3: (a) The relationship between phase shift on reflection from a DBR mirror and the wavelength being reflected. (b) The relationship of how EQE depends on both the top mirror reflectivity (number of layer repeats) and absorber thickness, for 13 repeats of lower DBR and an InGaAsSb absorber.

As photodetectors, RCE-PDs generate their signal from absorption of the light in the cavity. This absorption is a damping effect and successful design must carefully optimise the magnitude of absorption to avoid excessive damping. If resonance is excessively damped, coupling of light into the cavity will be reduced, concomitantly reducing external quantum efficiency (EQE). However, optimisation is not simply a case of maximising the cavity quality (Q) factor and hence coupling into the cavity, since some absorption is necessary to generate signal. Figure 3 (b) shows an example of the trade-off to be made between the number of top mirror repeats (reflectivity), absorber thickness, (damping and signal generation) to maximise EQE. With appropriate design >80% EQE is achievable.

2.2   Temperature Stability

For conventional broadband detectors the detector cut-off wavelength is defined by the bandgap energy of the absorbing material. This bandgap energy has a non-negligible temperature dependence, leading to a spectral response which changes with temperature. Because the spectral response of RCE-PDs is primarily defined by the DBR mirrors and the optical path length of the $\lambda/4$ thick DBR layers, changes to this path

length define the temperature dependence of the spectral response. In practice, it has been shown that the temperature dependence of the refractive indices is the dominant factor defining the shift in resonance wavelength, with thermal expansion only having a secondary effect. Overall, the resonance wavelength is much less dependent on temperature than the bandgap energy defined cut-off wavelength of a broadband detector, as shown in Figure 4(b). However, if the detector is likely to experience large changes in temperature, it is important to note that the absorption coefficient can change sufficiently with temperature to affect the designed Q-factor and hence the EQE. Figure 4(a) shows an extreme example of this effect in an RCE-PD. In this case the bandgap of the InAs absorber is approaching the resonance photon energy, at the lower temperatures, and hence the absorption coefficient is reducing significantly, decreasing the EQE dramatically.
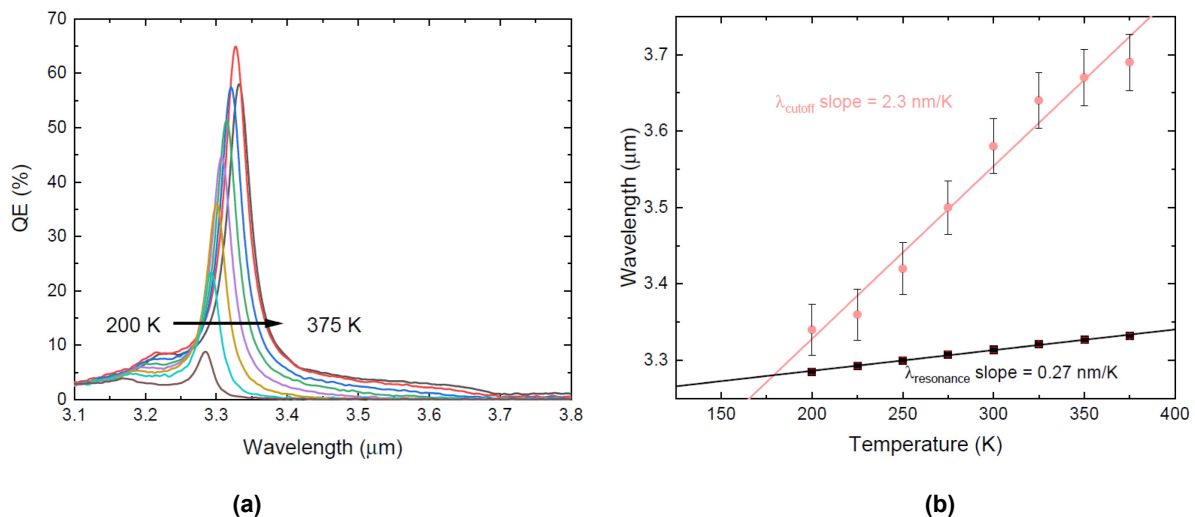
Figure 4: (a) Temperature dependent spectral response of an RCE-PD with InAs absorber, illustrating the effect of a significantly varying absorption coefficient. (b) The shift in resonance wavelength and bandgap cut-off for the same RCE-PD and InAs absorber, illustrating the greatly reduced shift for the RCE-PD.

2.3   Enhancement of Detectivity

To achieve acceptable quantum efficiency (signal), conventional infrared detectors require an absorber with a thickness on the order of the free-space wavelength being detected. For a well-designed detector, this volume of narrow-gap semiconductor gives rise to the majority the detector's leakage current (noise). Hence there is an inherent concomitance of signal and noise generation in conventional infrared detectors, which limits achievable detectivity (D*), particularly when uncooled or minimally cooled. RCE-PDs can achieve high EQE with a one to two orders of magnitude lower thickness of the narrow bandgap material, due to their enhancement of the optical field. The re-writes the conventional link between signal and noise generation, increasing the fundamentally limited D*. Furthermore, the spectral selectivity of the cavity rejects broadband background radiation and it has already been shown experimentally that this raises the fundamental BLIP limit [9]. Figure 5(a) shows an example of the reduction in leakage current achieved in an RCE-PD based on an InAs absorber, compared to a conventional InAs nBn detector; greater than one order or magnitude above room temperature. As evident in the figure, scaling the leakage in proportion to the absorber thickness can be difficult to achieve, particularly at low temperatures where interface effects can dominate over the scalable bulk material leakage generation. Overall, RCE-PDs have been shown to achieve enhanced D* figures of merit.[10] Figure 5(b) shows how the same InAs based RCE-PD can achieve a D* as high as 10^{10} Jones, even at an elevated temperature of 350K.
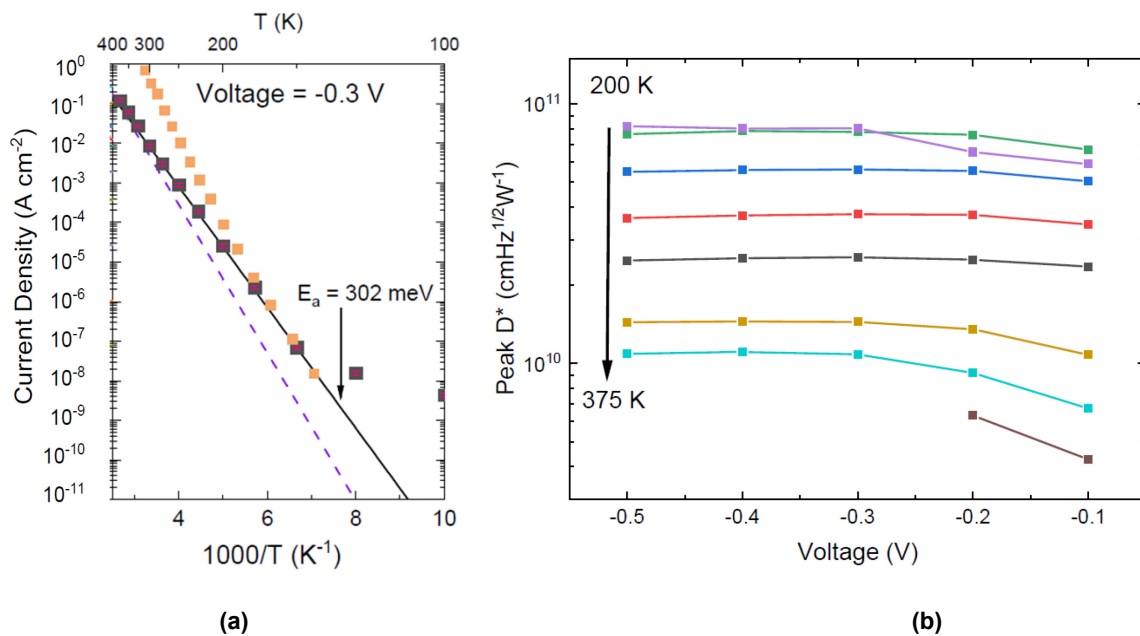
Figure 5: (a) Arrhenius plot showing suppression of leakage current in an RCE-PD with an InAs absorber and ~3.3 μm resonance wavelength (black), compared to a conventional InAs nBn (orange) and approaching Rule 07 (purple) at high temperatures. (b) D* for the same ~3.3 μm RCE-PD, biased at 0.3V, for temperatures between 200K and 375K in 25K steps.

3.0   TECHNOLOGIES TO COVER THE IR SPECTRUM

RCE-PD development has benefited from the work in recent decades to develop a family of materials, lattice matched to GaSb, which can act as the absorbers in IR detectors. InGaAsSb can be used for cut-off wavelengths up to ~2.8 μm at 300K, InAsSb for a cut-off wavelength of ~4.5 μm at 300K and InAs/GaSb or InAs/InAsSb superlattices for cut-off wavelengths up to at least 12 μm at cryogenic temperatures. Between them, these materials effectively cover the highlighted 1.5 – 12 μm range, relevant to spectroscopic material sensing. RCE-PDs have been realised using all these absorber materials and AlAsSb/GaSb DBR mirrors [8]-[11]. However, there is a significant reduction in bandgap between the miscibility gap limit of InGaAsSb and the fixed lattice matched composition of InAsSb. This jump coincides with the ~0.37 eV photon energy which excites resonance in the very common C-H bond. For this reason researchers have demonstrated RCE-PDs exploiting an InAs absorber, which has an essentially optimal bandgap for sensing 0.37eV photons with maximal detectivity [12]. These InAs based RCE-PDs use a lattice matched AlAsSb/GaAsSb DBR mirror technology. Example epitaxial layer structures are shown in Figure 6, for RCE-PDs on GaSb and InAs substrates. In both cases the detectors shown employ an nBn detector architecture inside a λ/2 wide cavity between DBR mirrors. Figure 7 shows spectral responses collected from a range of RCE-PDs created at Lancaster University, with the absorber material used in each spectral region highlighted. In addition to these a longwave IR sensitive RCE-PD has been realised, detecting at 7.7 μm.[13]

Based on rapid progress over the last 6 years in particular, RCE-PDs have now been developed to detect across a wide range of the IR spectrum, relevant for chemical or explosive threat detection. They can be designed to target an absorption line with as little as 10nm FWHM, and achieve this in a sub-mm sized chip operating photovoltaically. Without the need for separate filters, gratings, moving mirrors or high-power lasers, they have the potential to be integrated into ultra-portable and robust detectors for use in any environment.

| 5 x 166.4 nm AlAs$_{0.08}$Sb$_{0.92}$ |
| 6 x 138.1 nm GaSb |
| 30 nm InAs$_{0.91}$Sb$_{0.09}$ |
| 30 nm In$_{0.25}$Ga$_{0.75}$As$_{0.22}$Sb$_{0.78}$ |
| 60 nm Al$_{0.36}$Ga$_{0.64}$Sb |
| 60 nm In$_{0.25}$Ga$_{0.75}$As$_{0.22}$Sb$_{0.78}$ |
| 136 nm AlAs$_{0.08}$Sb$_{0.92}$ |
| 13 x 166.4 nm AlAs$_{0.08}$Sb$_{0.92}$ /138.1 nm GaSb |
| GaSb Substrate |

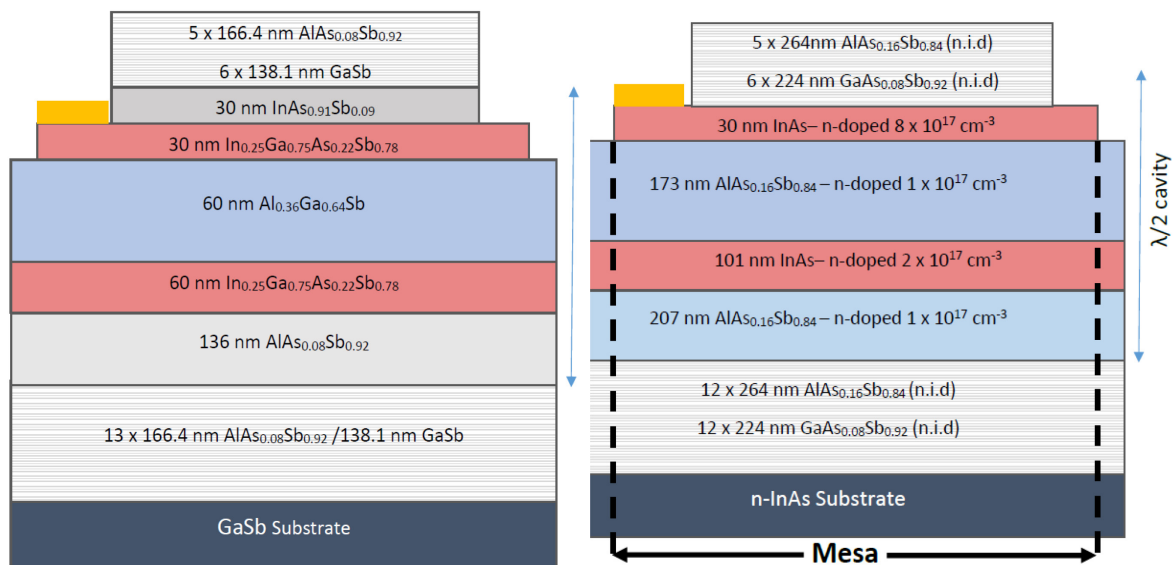| 5 x 264nm AlAs$_{0.16}$Sb$_{0.84}$ (n.i.d) |
| 6 x 224 nm GaAs$_{0.08}$Sb$_{0.92}$ (n.i.d) |
| 30 nm InAs– n-doped 8 x 10^{17} cm^{-3} |
| 173 nm AlAs$_{0.16}$Sb$_{0.84}$ – n-doped 1 x 10^{17} cm^{-3} |
| 101 nm InAs– n-doped 2 x 10^{17} cm^{-3} |
| 207 nm AlAs$_{0.16}$Sb$_{0.84}$ – n-doped 1 x 10^{17} cm^{-3} |
| 12 x 264 nm AlAs$_{0.16}$Sb$_{0.84}$ (n.i.d) |
| 12 x 224 nm GaAs$_{0.08}$Sb$_{0.92}$ (n.i.d) |
| n-InAs Substrate |

$\lambda/2$ cavity

Mesa

Figure 6: Examples of full RCE-PD epilayer structures. (Left) the widely applicable GaSb based technology using AlAsSb/GaSb DBRs. (Right) the InAs based technology using AlAsSb/GaAsSb DBRs, specifically suited to detection around 3 μm. Layer thicknesses not to scale.
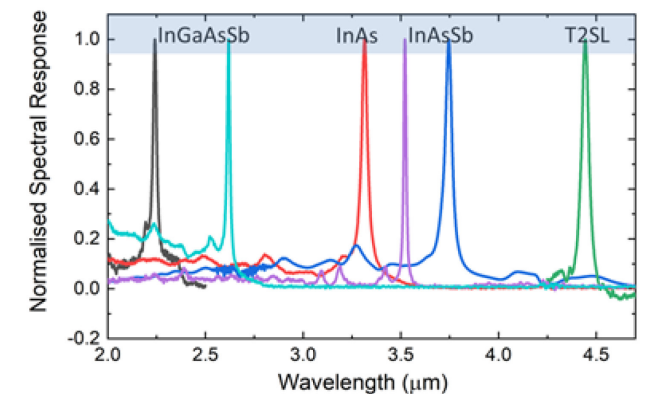
Figure 7: RCE-PD spectral responses for sample detectors, illustrating the range of absorber material technologies required to span the IR range of interest for threat detection. The FWHMs of the responses vary by design. Some devices are fabricated with a simple processing procedure which leaves low level broadband response. The purple response is indicative of the response purity which is achievable with refined design and processing.

4.0   SPECTROMETER ON A CHIP

Whilst RCE-PDs capable of selectively sensing a single narrow spectral bandwidth have potential applications in spectral sensing, they are realistically only suited to controlled environments or the detection of strong absorption features. For sensing in complexed environments or mixtures, it is necessary to collect detailed spectral information. It is clear that changing the layer thicknesses in an RCE-PD affords control over the resonance wavelength. As shown in Figure 8(a), it is easy to conceived of using multiple (N) RCE-PDs, with different layer thicknesses, to allow sampling of a spectrum at multiple wavelengths. It is far less trivial to achieved this in practice, without growing N distinct wafers and processing them into N distinct RCE-PD chips.

To realise a spectral sensing array of RCE-PDs without assembling one from multiple individual chips, a "chirped" RCE-PD array has been developed. With the aid of an inventive growth routine, the thickness of GaSb layers in the DBRs and the cavity have been graded along one axis, during epitaxial growth [14]. Linear arrays have been fabricated along this axis, with a single chip containing hundreds of individual RCE-PDs, each with a slightly different resonance wavelength. The "chirping" of the resonance wavelength with respect to position, across the central region of a single 2" diameter wafer, is shown in Figure 8(b). Figure 8(c) shows measurement results obtained using a linear array processed from the same wafer. The array was used to characterise the emission from a grating spectrometer, by measuring the photocurrent for each pixel. If integrated with an off-the-shelf linear array read out IC (ROIC), this data could be collected in milli or even microseconds. It is clear that 5nm steps in the output wavelength of the spectrometer are easily resolved by changes in the measured photocurrent as a function of pixel number (position) along the array. Using this data, spectral reconstruction has been demonstrated and we estimate the accuracy to be $\sim \pm 1$ nm in this first proof of concept. Refinements to achieve sub-nm resolution would be straightforward to implement in a future project. In on-going research, data processing algorithms are being applied to the output of larger arrays, aiming to demonstrate extended spectral recreation and detection of mixtures and threats in complexed environments.


(a)

(b)

(b)
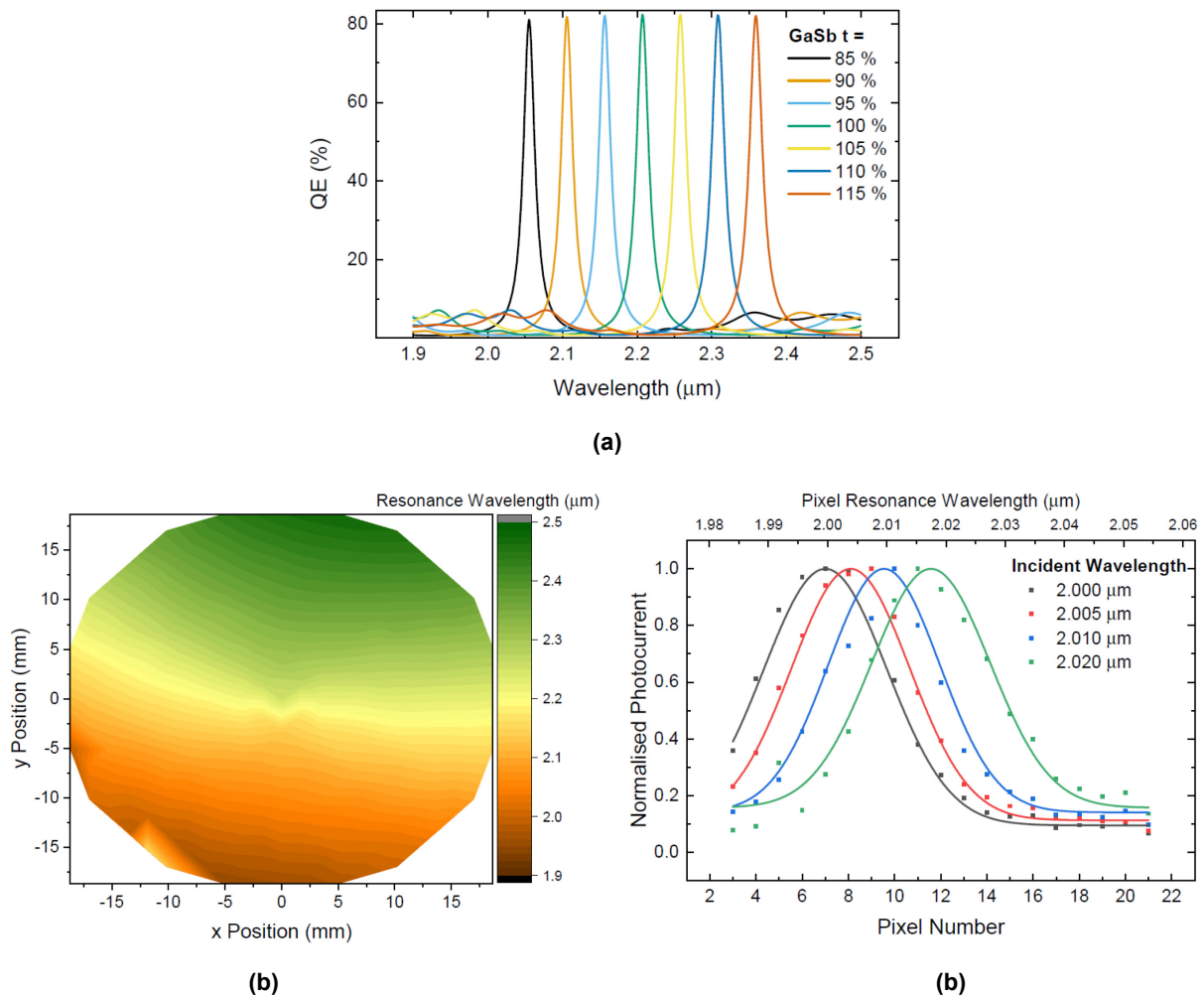
Figure 8: (a) Simulated spectral responses, illustrating the concept of varying layer thickness (t) to produce an array of RCE-PDs sensing at different wavelengths on a single chip. (b) Transmission mapping of the resonance wavelength as a function of position, for a 2" diameter wafer grown with thickness grading along a defined axis. (c) Characterisation of a spectrometer output, using a "chirped" array of RCE-PDs fabricated from the wafer shown in (b).

5.0   INITIAL APPLICATION TRIALS

Outside the laboratory environment, infrared absorption spectroscopy is most commonly applied to detect gasses, which give the clearest absorption lines because their molecules, and hence bond resonances, exist in effective isolation. Within liquids, absorption lines are broadened and overall medium absorbance is often high, presenting a greater challenge. To advance application of RCE-PD based spectral sensing and investigate a challenging application sensing in a liquid mixture, our group has been evaluating the optical detection of low glucose concentrations in water.

Water is a complexed medium to sense within, exhibiting positive and negative displacement factors with solutes like glucose, and positive and negative temperature coefficients for its own absorbance. The concept being trialled is illustrated in Figure 9. The combined effect of glucose absorption (combination band) and water displacement, results in a maximum dependence of absorbance on glucose concentration around a wavelength of ~2.14 um. Due to the highly absorbing medium, a single sensing channel will interpret even small path length changes as a large change in glucose concentration. To combat this a second control channel is essential. Fortunately, around a wavelength of ~ 2.24 um, combined absorbance is insensitive to changes in glucose concentration, providing an ideal control.
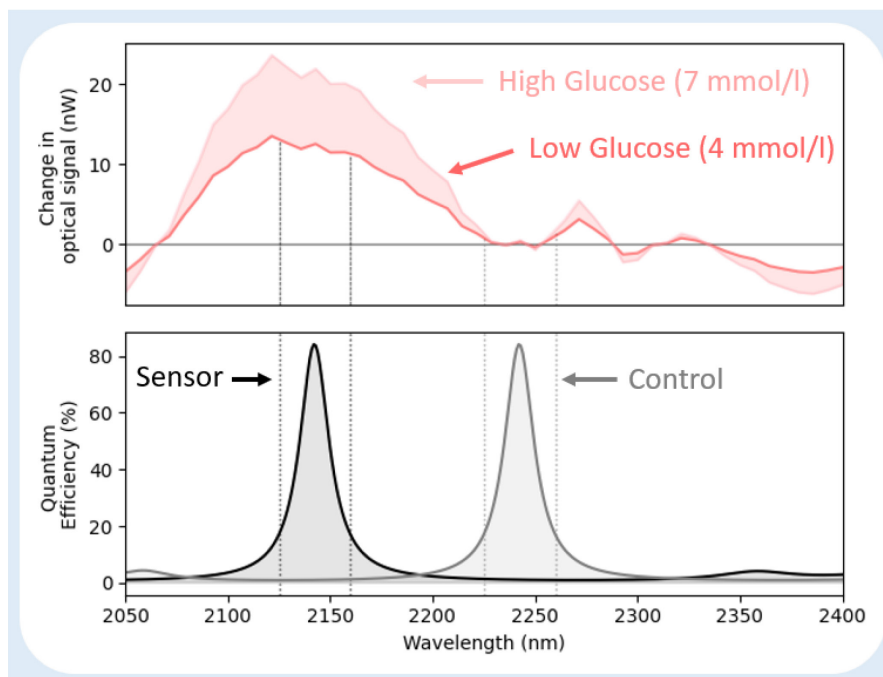
Figure 9: The glucose-water mixture concept being trialled as a testbed for implementing RCE-PD spectral sensing. (Top) Calculated change in optical power after passing through glucose concentrations with concentrations considered healthy for human blood. (Bottom) Simulated RCE-PD responses designed to align spectrally with the maximum change and a control wavelength respectively.

As shown in Figure 9, the absolute change in optical power expected due to human-relevant changes in glucose concentrations, with respect to pure water, is on the order of 10 nW. This calculation assumes a simple LED launches 1 mW of optical power into the medium. Moreover, the fractional change in the optical power reaching the sensors is small, requiring >10 bits of resolution to detect. Although small, this change is comparable that exploited in photoplethysmography, so well within the resolution of ACDs widely applied in consumer wearables. These challenges and attributes make this application a good testbed for system level proof of concept. The obvious complementary motivation being that cheap, non-invasive optical sensing of

glucose levels would improve the life of hundreds of millions of diabetics worldwide. To date, detection of glucose concentrations in the healthy 4 – 7 mmol/l range has been achieved, but there remains significant scope for improvement and system lessons to be learnt. The experience gained can be applied to future threat detection systems based on RCE-PDs

6.0   CONCLUSIONS

Broadband IR detectors have evolved relatively minimally over recent decades, whilst at the same a tremendous research effort has advanced IR emitter technology significantly. The development of IR RCE-PDs goes some way to redress this imbalance, applying advanced optical design and epitaxial techniques to produce a compelling new detector technology. Integrating spectral selectivity into the detector allows simple spectroscopic threat detection to be designed with minimal components and low size and power requirements. In the limit a single RCE-PD chip, operated in combination with a single LED chip, each sub-mm in size, could form a simple detection system. Furthermore RCE-PDs have enhanced detectivity and temperature stability compared to broadband detectors, boosting system sensitivity or allow cooling to be reduced or removed. The demonstration of this new capability in testbed systems is ongoing, including the use of a novel integrated linear array of RCE-PDs, achieving spectrometer level spectral resolution on a chip.

7.0   REFERENCES

[1]   Coblentz Society. Evaluated Infrared Reference Spectra. eng. Gaithersburg MD, 20899: National Institute of Standards and Technology, 2012. ISBN: 012387839X.

[2]   N. Pelin Ayerden and Reinoud F. Wolffenbuttel. "The Miniaturization of an Optical Absorption Spectrometer for Smart Sensing of Natural Gas". In: IEEE Transactions on Industrial Electronics 64.12 (2017), pp. 9666–9674.

[3]   Mohammad Sadegh Faraji-Dana et al. "Compact folded metasurface spectrometer". In: Nature Communications 9.1 (2018), p. 4196.

[4]   Zongyin Yang et al. "Single-nanowire spectrometers". In: Science 365.6457 (2019), pp. 1017–1020.

[5]   Brandon Redding et al. "Compact spectrometer based on a disordered photonic chip". In: Nature Photonics 7.9 (2013), pp. 746–751.

[6]   M. Selim Ünlü and Samuel Strite. "Resonant cavity enhanced photonic devices". In: Journal of Applied Physics 78.2 (1995), pp. 607–639.

[7]   Alex M Green et al. "∼ 3μm InAs resonant-cavity-enhanced photodetector". In: Semiconductor Science and Technology 18.11 (2003), pp. 964–967.

[8]   Trevor A. O'Loughlin et al. "Mid-IR resonant cavity detectors". In: Journal of Vacuum Science & Technology B 35.2 (2017), 02B111.

[9]   Veronica Letka et al. "Resonant cavity-enhanced photodetector incorporating a type-II superlattice to extend MWIR sensitivity", Optics Express, vol. 27, no. 17, pp. 23970-23980.

[10]   Adam P. Craig et al. "Resonant cavity enhanced photodiodes on GaSb for the mid-wave infrared", Applied Physics Letters, vol. 114, no. 15, 151107.

[11] Andrew Bainbridge et al. "Resonant Cavity Enhanced Photodiodes in the Short-Wave Infrared for Spectroscopic Detection", IEEE Photonics Technology Letters, vol. 32, no.21, pp. 1369-1372.

[12] Andrew Bainbridge et al. "Resonant Cavity–Enhanced Photodiodes for Spectroscopy of C-H Bonds", physica status solidi (a).

[13] Veronica Letka et al. "A superlattice based resonant cavity-enhanced photodetector operating in the long-wavelength infrared', Applied Physics Letters, vol. 117, no. 7, 073503.

[14] Andrew Bainbridge et al. "Resonant Cavity-Enhanced Photodiode Array for Miniaturised Spectroscopic Sensing', Optics Express, vol. 30, no. 3, pp. 3230-3237.